# A Theoretical Investigation of the Mechanisms of Fracture in Metals and Alloys

**M. E. Eberhart,*,† D. P. Clougherty,‡ and J. M. MacLaren§**

*Contribution from the Department of Metallurgical and Materials Engineering, Colorado School of Mines, Golden, Colorado 80401, Department of Physics, University of Vermont, Burlington, Vermont 05405-0125, and Department of Physics, Tulane University, New Orleans, Louisiana 70118*

*Received July 27, 1992*

**Abstract:** A fundamental understanding of the atomic mechanisms responsible for the stress-induced bond failure of solid-state materials will facilitate the synthesis of materials with desired mechanical properties. Outside of a small group of network solids and polymers, no such understanding is available. By adopting an appropriate model for solid-state bonding, based on features of the total charge density, it is possible to apply chemical reaction theory to an investigation of this process. First-principle local-density-functional techniques were used to model the transgranular fracture of two alloys with the same crystal structure but different mechanical properties, a hitherto unexplained observation. It was found that the transition state for decohesion occurs earlier in the reaction path for the brittle than for the ductile alloy. This observation is argued to be the result of a comparatively flat charge density at a few special points within the alloy. The success found in the application of reaction theory toward an understanding of decohesion suggests that reaction theory might be profitably employed in more complex and technologically important investigations of mechanical properties of solids.

## 1. Introduction

Fracture, corrosion, and wear are problems of tremendous scientific, technological, and economic concern. At the most fundamental level, each of these phenomena is the result of stress-induced rupture of cohesive bonds. Despite the interest in these phenomena, a representation of the chemical mechanism by which these bonds fail is restricted to only a few materials. In the largest class of structural materials, metals and alloys, there is no such description. As a result, the synthesis of metallic materials with desired intrinsic mechanical properties proceeds through empiricism. A rationale which allows for the systematic alteration of these properties would have potentially far-reaching beneficial consequences.

Modern reaction theory provides a well-established formalism for analyzing atomic scale interactions. There is no a priori reason that this same formalism can not be generalized to the study of the stress-induced failure of chemical bonds. Consequently, we report here on our efforts to extend reaction theory toward an understanding of intrinsic mechanical properties of condensed-phase systems, with particular emphasis on metals and alloys.

Of all the intrinsic mechanical properties, perhaps the technologically most significant in metallic systems is related to the competition between ductile and brittle behavior. Whether a material responds to loading in a ductile or brittle fashion is understood to be related to atomic interactions at the tip of microcracks which occur naturally in most materials (Figure 1). When a material is loaded (in our example in tension), the stress at the tip of the crack can exceed the average stress in the material. How the material responds will depend intimately on the state of stress at the tip of this crack. The two components of the stress which must be considered are the resolved shear stress on the planes inclined to the crack and the tensile stress across the crack. If the tensile stress is greater than the bond strength (the theoretical cohesive strength) at the crack tip, the crack will extend. With the lengthening crack, the stress concentration at the tip increases; the bonds here become unstable and the crack begins to run. This

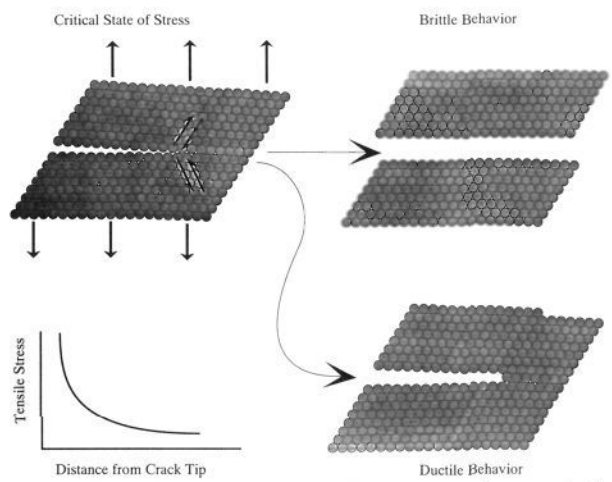


**Figure 1.** Stress distribution at the tip of an atomically sharp crack. The tensile stress intensity along the plane of the crack (graph) is a function of the crack length and the crack tip curvature. The stress intensity at the crack tip can not exceed either the ultimate tensile strength across the crack plane or the ultimate shear strength on the planes inclined to the crack surface. If the ultimate tensile strength is exceeded first, the crack will run, resulting in fracture. This behavior is typical of a brittle material. If the ultimate shear strength is exceeded first, a dislocation will nucleate, blunting the crack tip and reducing the stress intensity. This behavior is characteristic of a ductile material.

is the situation in materials which fail in a brittle fashion, silica glass being a familiar example. Alternatively, the resolved shear stress at the crack tip can also exceed the theoretical shear strength of the material. In such a case, a dislocation will nucleate, i.e. slip. This will blunt the crack and the stress concentration at the tip will decrease. Materials which behave in this manner are ductile. Many simple metals fall into this class such as Cu, Fe, and Ni. Ductile versus brittle behavior can thus be seen to be a competition between decohesion and slip.

Ductile behavior is often preferred in structural materials, and consequently, the first step in the design of a structural material is concerned with inducing ductile behavior. In many intermetallic compounds, the intrinsic failure modes are brittle and much effort

† Colorado School of Mines.
‡ University of Vermont.
§ Tulane University.

0002-7863/93/1515-5762$04.00/0 

is expended in identifying alloying elements which will induce ductile behavior. Unfortunately, this process proceeds empirically.

One might think of ductile and brittle behavior as being competing reactions, that is, slip competing with decohesion. Reaction theory provides a well-established formalism for approaching problems of competing reactions. To promote ductile behavior, one would provide a chemical environment which will stabilize the transition state for slip. On the other hand, to promote brittle behavior, an environment which stabilizes the transition state for decohesion will be required.

Consider the two alloys CuAu and TiAl. These alloys share the same crystallographic structure, yet have different mechanical properties. CuAu is ductile while TiAl is brittle. One explanation for this difference in properties is that, of the two alloys, the transition state for decohesion is reached earlier in TiAl. The problem associated with testing this hypothesis involves identifying the transition state for decohesion. Unfortunately, the arrangement of the atoms at the transition state is unknown for both alloys. With this state of knowledge, it is impossible to apply reaction theory to this process and thus test the hypothesis.

Typically, the problems encountered above are overcome by comparing the *bonding* of the reactants and products to that of the transition state. These comparisons are conducted within the most appropriate model for the systems of interest, e.g. the Lewis model for organic reactions or molecular orbital models for coordination complexes. Therefore, before one can apply transition state theory to a study of mechanical behavior, one must first develop a formalism for describing the bonds in condensed matter systems and in particular metals and alloys.

A description of bonding which has the potential to describe both molecular and solid-state bonding has been outlined in a series of papers by Bader.[1-5] The framework proposed is empirical in nature, but it has faithfully reproduced conventional descriptions of molecular bonding; it produces the same topological features of the bonding between atoms in a molecule as the conventional valence bond or Lewis approach. As this method is based on features of the total charge density, there is no reason to assume that it should not be fully generalizable to different types of bonding in different classes of materials. The fact that bonds can be described by features of the total charge density is particularly appealing, as the total charge density is experimentally accessible through X-ray diffraction studies and one of the principal results of electronic structure calculations. In addition, the ground state charge density is in principle exactly calculable by techniques which solve the Kohn–Sham equations.

The calculations of the charge densities which follow were performed using the layer Korringa–Kohn–Rostoker (LKKR) method.[6,7] While any electronic structure technique could have been used, since charge density is physically observable and should be method-independent, the approach adopted here is particularly suited to the low-symmetry environments found at interfaces.

## 2. Bonds in Metals

The charge density is a scalar field, $\rho(\vec{r})$, which as with any scalar field possesses a unique topology. This topology is characterized in terms of its critical points, which are defined as the zeros of the gradient of the scalar field. There are four kinds of critical points in a three-dimensional space: a local minimum, a local maximum, and two kinds of saddle points. These critical points (cps) are denoted by an index which is the number of positive curvatures minus the number of negative curvatures. For example, a minimum cp has positive curvature in the three orthogonal directions; therefore, it is called a (3, 3) cp, where the first number is simply the number of dimensions of the space, and the second number is the net number of positive curvatures. A maximum would be denoted by (3, −3), since all three curvatures are negative. A saddle point with two of the three curvatures negative is denoted (3, −1), while the other saddle point is a (3, 1) cp.

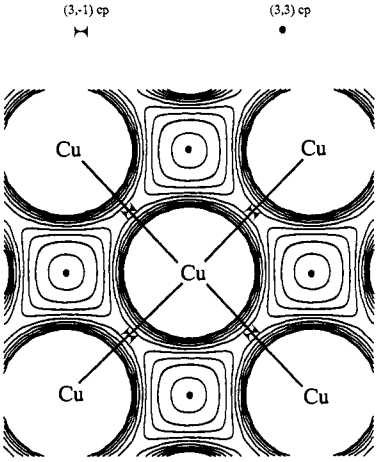


**Figure 2.** Charge density in the (100) plane of copper with critical points marked by type. The (3, −1) cps designate the Cu–Cu bonds while the (3, 3) cps are a necessary feature of the octahedral bonding polyhedra.

The classification of molecular charge density in terms of the positions of the critical points of the charge density, i.e. its topology, has been shown to reproduce much of what we consider chemical structure. Bader realized that a bond in molecules can be seen in terms of the topology of $\rho(\vec{r})$.[1-5] A bond path connects two nuclei (where the charge density possesses (3, −3) cps) through a (3, −1) cp such that the charge density is always a maximum with respect to any neighboring path. Other types of critical points have been correlated with other features of molecular structure. A (3, 1) cp is seen at the center of planar ring structures like benzene. Accordingly, this critical point has been designated as a ring critical point by Bader. Cage structures are always characterized by a single (3, 3) cp somewhere within the cage, and again have been given the descriptive name of cage critical points. Many of these ideas have recently been extended to the solid state, where the notion of the metallic bond was discussed.[8,9]

The charge density topology is fully determined by the positions and type of critical points. As the location of nuclei in a crystal will always correspond to a maximum in the charge density, a (3, −3) cp, the structure of the charge density caries more information than does the crystal structure alone. This additional information is related to the "connectedness" of the atoms in a particular crystal structure. Thus two identical crystal structures need not show similar charge density topologies, as it is possible to connect the atoms in a number of different ways.

Figure 2 shows the positions and type of critical points in a (100) plane of Cu. This topology is characteristic of all fcc allotropic metals we have modeled, and therefore, we designate this as an fcc topology. The (3, −1) cps midway between nearest neighbors are indicative of bonds between these atoms, which are shown as lines connecting the bound atoms. These bonds form additional 2D and 3D structures within the crystal which in turn necessitate the existence of additional critical points. In particular, these bonds are the edges of two types of polyhedra or cages:

(1) Bader, R. F. W.; Preston, H. J. T. *Int. J. Quantum Chem.* **1969**, *3*, 327.
(2) Bader, R. F. W.; Beddall, P. M.; Peslak, J., Jr. *J. Chem. Phys.* **1973**, *28*, 557.
(3) Runtz, G. R.; Bader, R. F. W.; Messer, R. R. *Can. J. Chem.* **1977**, *55*, 3040.
(4) Bader, R. F. W.; Nguyen-Dang, T. T.; Tal, Y. *Rep. Prog. Phys.* **1981**, *44*, 893.
(5) Bader, R. F. W.; MacDougall, P. J. *J. Am. Chem. Soc.* **1985**, *107*, 6788.
(6) MacLaren, J. M.; Crampin, S.; Vvedensky, D. D.; Pendry, J. B. *Phys. Rev. B* **1989**, *40*, 12164.
(7) Crampin, S.; Vvedensky, D. D.; MacLaren, J. M.; Eberhart, M. E. *Phys. Rev. B*, **1989**, *40*, 3413.
(8) Eberhart, M. E.; Clougherty, D. P.; Lowen, J. *Mater. Res. Bull.* **1991**, 53.
(9) Eberhart, M. E.; Donovan, M. M.; MacLaren, J. M.; Clougherty, D. P. *Prog. Surf. Sci.* **1991**, *36*, 1.

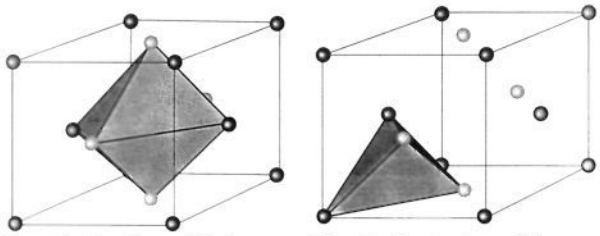

**Figure 3.** Bonding polyhedra comprising the fcc structure. These are {6, 12, 8} (left) and {4, 6, 4} (right) polyhedra. These polyhedra alone determine the *topology* of the fcc charge density.

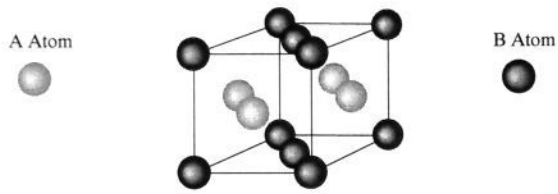


**Figure 4.** $L1_0$ structure. CuAu and TiAl share this structure.

tetrahedra and octahedra (Figure 3). At the center of each of these polyhedra is a cage critical point, i.e. a (3, 3) cp, with the octahedral cage critical points shown in Figure 2. At the center of each of the faces of these two polyhedra are ring critical points. The entire set of critical points defines specific bonding polyhedra, the packing of which gives rise to the fcc structure. The *topology* of these polyhedra is determined only by the number of corners, edges, and faces. As a convenience, we will adopt the notation {c, e, f} to designate a polyhedron. A polyhedron topologically equivalent to a regular tetrahedron will have four corners, six edges, and four faces, {4, 6, 4}. The total charge density will reflect these features with a (3, −3) cp at each corner, a (3, −1) cp along each edge, a (3, 1) cps in each face, and a (3, 3) cp within this polyhedron. The fcc topology is the result of packing two types of polyhedra, a {4, 6, 4} and a {6, 12, 8} (octahedra), with each face of the {4, 6, 4} shared with a {6, 12, 8}. Any structure whose charge density gives rise to the same set of bonding polyhedra, packed in the same manner, is topologically equivalent to the fcc structure.

Polyhedral models of structure have been widely used. Pauling[10] has used polyhedral models to describe the crystal structure of ionic solids, and Ashby et al.[11] have used a similar approach to describe grain boundary structure. In both of these examples, there is some ambiguity, however, in the way in which polyhedra are assigned. This ambiguity is eliminated when the natural features of the total charge density are used to identify bound atoms and the resulting bonding polyhedra.

**2.1 Bonding in the $L1_0$ Structure.** We turn now to a discussion of the charge density topology in two alloy systems with the same crystal structure, $L1_0$, but different mechanical properties. The $L1_0$ structure is fcc derived and is characterized by alternating planes of all A atoms and all B atoms. It is shown schematically in Figure 4. The two representative alloys investigated here are CuAu and TiAl. Though they share the same structure, their mechanical responses are quite different. CuAu is the archetypal ductile intermetallic, showing no ductile–brittle transition (DBT) even at cryogenic temperatures. Intrinsic failure in this alloy always occurs with a ductile morphology. CuAu undergoes an order–disorder transition at temperatures above 410 °C, where the disordered $L1_0$ state is fcc. TiAl, on the other hand, is extremely brittle, failing by transgranular cleavage at temperatures below the ductile–brittle transition temperature of 700 °C with no discernible elongation. This failure has been attributed to intrinsically weak cleavage planes. TiAl is ordered to the melting point.

(10) Pauling, L. *J. Am. Chem. Soc.* **1929**, *51*, 1010.
(11) Ashby, M. F.; Spaepen, F.; Williams, S. *Acta Metall.* **1978**, *26*, 1647.

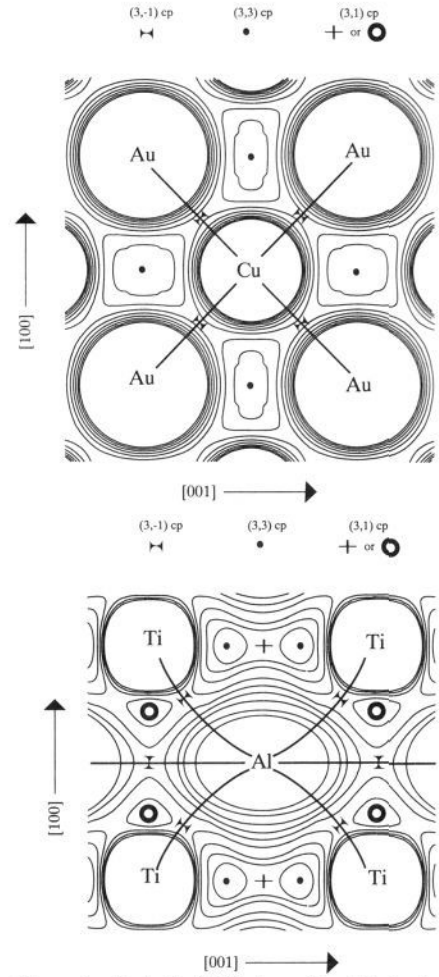


**Figure 5.** Charge density in the (100) plane with critical points identified by type for (top) CuAu and (bottom) TiAl. Here the symbol for a ring critical point designates the plane of the corresponding ring. (top) The topology of this charge density is identical to that of Cu in Figure 1. (bottom) This charge density topology is "richer" than that of CuAu, with both a second-neighbor bond between Al atoms and a ring critical point, a (3, 1) cp, denoting the four-member Al rings in the (001) planes of all Al atoms.

Though CuAu and TiAl share the same crystal structure, these alloys possess different charge density topologies. The differences are best illustrated by plotting the charge density in the (100) planes (Figure 5). The tetragonal $L1_0$ structure is characterized by a c/a ratio of 0.94 for CuAu and 1.02 for TiAl. This tetragonal distortion produces a 2-fold rotational axis in these planes, as is clearly evident in the computed charge densities.

The charge density for CuAu shows a topology which is characteristic of fcc metals. There are four (3, −1) cps shown in this plane, one between each set of nearest neighbor atoms. This is indicative of first-neighbor bonds between these atoms. The bond paths are again shown as lines connecting the bound atoms. Note that for CuAu these are straight lines with the (3, −1) cp occurring near the midpoint of each of these bonds. On the axis between second-neighbor atoms, there is a (3, 3) cp, a cage critical point, which designates the bonding polyhedra topologically equivalent to the fcc octahedra. This is not a symmetry-imposed restriction as in the case of fcc metals. While not shown, the charge densities in (001) and (002) planes possess the same topology as that of the (100) plane. That is, the number and character of the critical points are identical. Thus the CuAu structure arises from bonding of nearest neighbors only, forming the two bonding polyhedra characteristic of the fcc structure. CuAu is, therefore, *topologically* fcc.

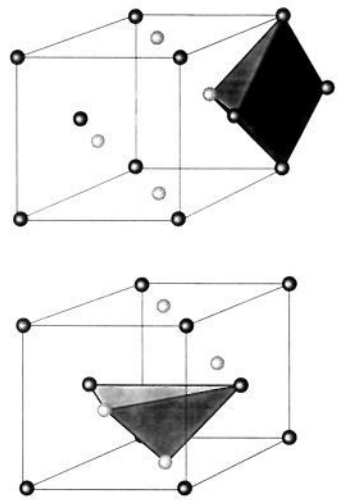

**Figure 6.** Two of the bonding polyhedra comprising the TiAl structure. These are {5, 8, 5} (top) and {4, 6, 4} (bottom) polyhedra. The topology resulting from the packing of these polyhedra is distinct from that of the fcc structure shown in Figure 2.

The computed charge density for TiAl in the (100) plane shows the four near-neighbor bonds between the Al atom and the Ti atoms. The (3, −1) cps corresponding to these bonds do not occur on the internuclear axes. The point is displaced off this axis and nearer the Ti atom, producing a bent bond path, i.e. a "banana" bond. There are additional critical points in this plane. One of these lies between second-neighbor Al atoms along the [001] direction. This point is a (3, −1) cp, corresponding to a bond between second-neighbor Al atoms. Another is a (3, 1) cp approximately a quarter of the way along the [100] direction between Ti atoms. This is a ring critical point designating a face of a {4, 6, 4} polyhedron, with the second-neighbor Al–Al bond, the first-neighbor Ti–Ti bond, and the four Ti–Al bonds defining the edges of this polyhedron (Figure 6). Four of these polyhedra pack to fill the same space that was filled in CuAu by a single {6, 12, 8} polyhedron. The other "octahedral hole" is also different than in CuAu. Where there was a (3, 3) cp in CuAu, there is a (3, 1) cp, a ring critical point, corresponding to one face of a bonding polyhedron characterized by the (3, 3) cp near the Ti atom along the [001] direction. This critical point corresponds to a {5, 8, 5} polyhedron, a square pyramid. Two of these polyhedra share square faces to fill the same space that was occupied by a single octahedron in CuAu. Obviously the charge density topology of TiAl is distinct from that of CuAu and is topologically inequivalent to the fcc structure.

**2.2 The Transition State for Decohesion.** By associating the transition state with the charge density topology at the point of topological instability, we are now in a position to identify the nature of the bonding at the transition state for decohesion. This is possible because for any sufficiently large tensile strain a free surface must be formed. Not all charge density topologies are compatible with free surfaces, and certain critical points must change their character as a component part of the formation of a free surface.

We begin to demonstrate these facts by first differentiating between two important 2D structures which are needed for a complete description of the evolution of the critical points of the charge density during fracture. The first of these is the fracture plane. The fracture plane is the plane of zero atomic density around which the two half spaces of the crystal separate during the fracture process. When these two half crystals are infinitely separated, the charge on this plane must be zero and the charge must increase away from this plane. Hence, on any line normal to the fracture plane, the charge must have positive curvature. However, on lines contained in the plane, the charge must be flat and zero. The second term is the fracture surface. This is simply the surface of the separating half crystals. This surface can contain only bond critical points and ring critical points, and the atoms associated with these bonds and rings. Obviously a cage critical point cannot be located on a free surface, nor can ring or bond critical points where the ring or bond (to which this point corresponds) has a component normal to the fracture surface.

The nature of the transition state accompanying decohesion can now be anticipated. Consider the strain of CuAu in a [100] direction, creating a (100) and an identical (200) fracture surface. The fracture plane is the (400) plane. The only critical points on this plane are the (3, −1) cps corresponding to the Cu–Cu, Au–Au, and Cu–Au bonds. The (100) fracture surfaces contain the (3, −1) cps corresponding to the in-plane Cu–Au bonds and the (3, 3) cps corresponding to the minimum of the charge density in the octahedral holes of the $L1_0$ structure. These cage critical points are incompatible with a (100) surface, and hence there must be charge flow to this minimum as a component part of free surface formation. The flux of the charge density accompanying this process (free surface formation) is therefore one in which charge must flows from the (3, −1) cps in the fracture plane (corresponding to bonds across the cleavage plane) into the (3, 3) cps in the fracture surface. The topological instability, which we associate with the transition state, will occur when the curvature of the charge density on the line normal to the bonds across the cleavage plane at the corresponding (3, −1) cps is zero and when the curvature normal to the forming surface at the cage critical point is also zero.

In the case of TiAl, the fracture surfaces are again a (100) and an identical (200) surface, while the fracture plane is "approximately" the (400) plane. The critical points in the fracture plane are the (3, −1) cps corresponding to Al–Al, Ti–Ti, and Al–Ti bonds and the (3, 3) and (3, 1) cps of the {4, 6, 4} polyhedra of Figure 6. The fracture surfaces contain, in addition to the (3, −3) cps corresponding to the Ti and Al atoms, the (3, 1) cp of the ring critical point designating a polyhedral face *normal* to the forming free surface and the (3, 3) cage critical point of the square pyramidal bonding polyhedron. Both of these critical points are not allowed on a free surface and hence must transform before a (100) free surface can be formed. Here, the transition state will once again have zero curvature perpendicular to the (3, −1) cps corresponding to the bonds across the cleavage plane and zero curvature normal to the forming free surface at the ring critical point.

We wish to compare the two reactions, (100) free surface formation in CuAu and TiAl, to determine which of the two transition states is reached earliest in the reaction path. We can perform a computational experiment to determine this.

**2.3 Calculation of Critical Strain.** Using the LKKR method of electronic structure, it is possible to calculate the charge density redistribution and to determine at what strain the transition state is reached. Figure 7 shows the geometry used for these calculations. Six (100) planes were used to model the interface region. The potentials on planes one and six were held fixed at their bulk values and matched to semi-infinite bulk crystals; the potentials on all other layers were allowed to relax through a self-consistent process. The distance between layers three and four has been increased 20% over its bulk value. This amounts to a displacement of 0.039 89 nm in TiAl and of 0.039 66 nm in CuAu. This calculation accurately models the charge redistribution associated with the rigid separation of TiAl and CuAu, providing the charge redistribution is confined to the first two layers of forming surfaces.

Figure 8 shows the change in the character of the charge density along the perpendicular to the A–B bond path in the (100) planes of CuAu and TiAl, following the modeled strain pictured in Figure 6. These are the critical points from which electron density should

(12) The atomic units for curvature are electrons/bohr$^5$. This is a measure of bond directionality, which we will designate as a Hecker (Hk).

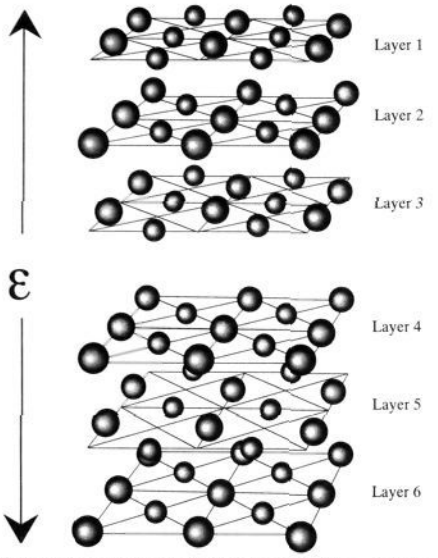


**Figure 7.** Geometry used in the LKKR calculations to determine the charge redistribution accompanying a localized strain between layers 3 and 4. This calculation accurately models the charge redistribution accompanying rigid separation of TiAl to the extent that the charge relaxation is confined to the first two surface layers.

flow as a part of the fracture process. A point of topological instability occurs when the charge is flat along this line at the bond critical point. Though in both alloys there is a net loss of density from these bonds, note that the (3, −1) cp of the Ti–Al bond across the cleavage plane has nearly vanished while in CuAu the character of the bond critical point, (3, −1), remains intact. Though not shown, the other (3, −1) cps in the cleavage planes of TiAl and CuAu are similar to those in Figure 8. The bonds in TiAl are broken or nearly broken whereas those in CuAu show only a small decrease in the curvature of the charge density at the critical point; their character remains the same.

Figure 9 compares the change in the charge density at the critical points located between the second-neighbor Ti (Au) atoms along [001] directions in the fracture surface. These are the critical points to which we anticipate the charge will accumulate if there is to be free surface formation. The plots of Figure 9 show the charge density along a line normal to the fracture surface. For both CuAu and TiAl, the curvature in this direction is positive; this is inconsistent with a free surface. In TiAl, as a result of the modeled strain, the character of the charge density along this line changes from a minimum to a maximum, producing a (3, −1) cp at this point, indicating the formation of a bond in the developing surface between second-neighbor Al atoms.

Thus for TiAl the point of topological instability and, we assume, the transition state are reached at or before 20% strain; however, in CuAu, the transition state is not reached at 20% atomic strain. We can conclude from this that, *of the two reactions, the decohesion of TiAl occurs earlier in the reaction path.*

While the strain at which the transition state for decohesion will be reached can be obtained from calculations, it would be advantageous to be able to compare the charge densities of the transition state with those of the reactants and products. To accomplish this we must develop a measure for the magnitude of a particular critical point.

The location of the cps is seen from the zeros of the gradient field of $\rho(\vec{r})$; the magnitude of these cps can be quantified by the value of the Hessian field of $\rho(\vec{r})$. The Hessian field is a tensor field given by $\mathcal{H}_{\alpha\beta}\rho(\vec{r}) = (\partial^2/\partial x_\alpha \partial x_\beta)\rho(\vec{r})$. When referred to principal axes, this is a diagonal tensor whose diagonal elements are the values of the curvature of the charge density in three orthogonal directions. With a quantification of the critical points of the charge density, it becomes possible to introduce the concept

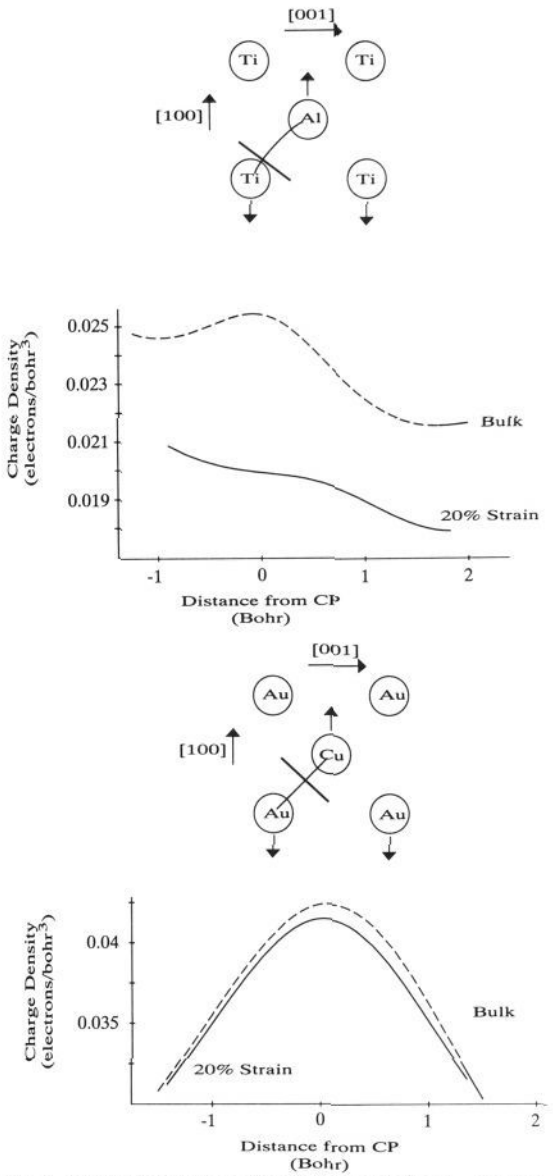


**Figure 8.** Charge density along the line normal to the (3, −1) cp (shown in the inset above each plot) for (top) TiAl and (bottom) CuAu as determined in the bulk and following 20% interatomic strain. These are the bonds which must break if this strain becomes sufficiently large. In TiAl the bond is broken at 20% strain whereas in CuAu it is not. The curvatures of the charge density along the plotted line evaluated at the critical points are bulk TiAl = −0.0079 Hk,[12] strained TiAl = −0.0001 Hk, bulk CuAu = −0.0160 Hk, and strained CuAu = −0.0165 Hk.

of "closeness" to a structural transition. For example, the structural transition which takes bulk TiAl to TiAl with a (100) surface requires the transformation of a (3, 1) cp to a (3, −1) cp. This is the result of a change from positive to negative curvature of one of the principal axes of the Hessian field, with the actual change in structure occurring as this axis develops a zero curvature, i.e. at the transition state. The greater the curvature of this principle axis the "further" topologically this crystal is from this structural transition. Thus the curvature of the axis undergoing a change in sign, as a component part of the change in structure, provides a measure of closeness to the transition state. Those systems, where the perpendicular components of the Hessian field of $\rho(\vec{r})$ evaluated at the critical point of the bonds being broken are near zero, are close to the transition state and thus have a high susceptibility to the reaction.

The component of the Hessian field of $\rho(\vec{r})$ for the relevant cps in TiAl and CuAu are given in the captions of Figures 8 and 9.

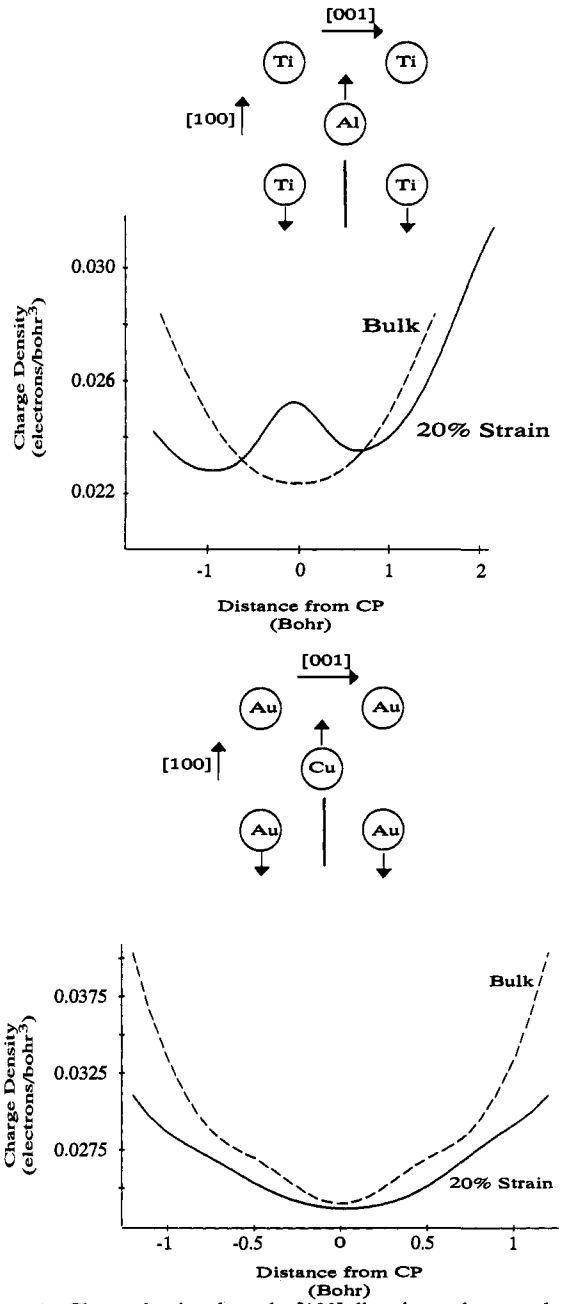


**Figure 9.** Charge density along the [100] direction and centered on the (3, 1) cp of (top) TiAl and the (3, 3) cp of (bottom) CuAu (shown in the inset above each plot as a heavy line). These are the critical points to which charge must flow if a free surface is to form. The curvatures of the charge density along the plotted line evaluated at the critical points are bulk TiAl = 0.0032 Hk, strained TiAl = −0.0089 Hk, bulk CuAu = 0.0320 Hk, and strained CuAu = 0.0113 Hk.

Note that for the bonds being broken and formed in TiAl the components of this field are nearer zero, the transition state, than those in CuAu. Thus, without the need to do the calculation to compute the strain at which the transition state will occur, it is possible to predict the relative susceptibility of TiAl and CuAu to decohesion. The transition state in TiAl will be reached earlier in the reaction path due to the nearness of the reactants to the transition state, and hence it is more susceptible to decohesion.

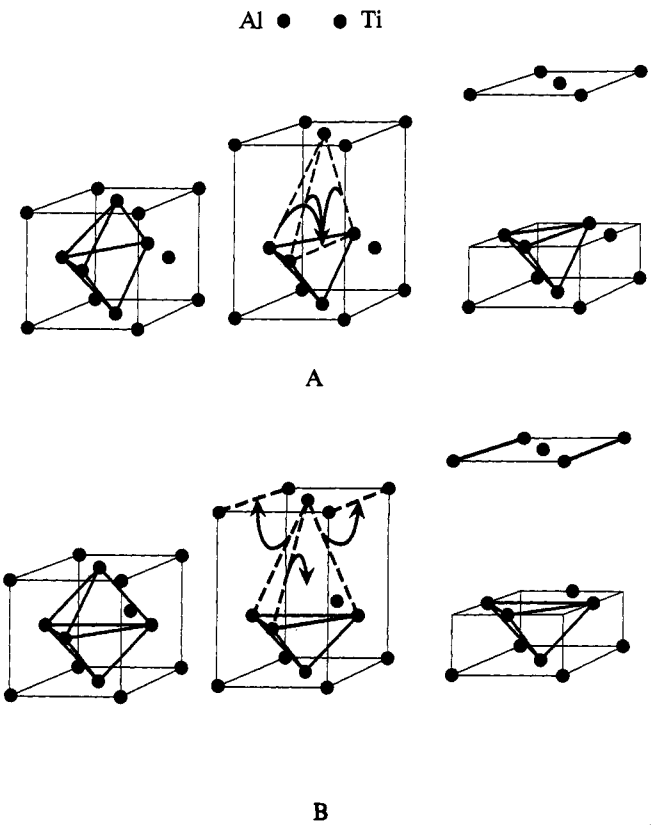


**Figure 10.** Summary of the charge redistribution accompanying (100) strain in TiAl. A shows the process accompanying the breaking of Ti–Al and Al–Al bonds, while B shows the charge redistribution accompanying the breaking of Ti–Ti bonds as well as Ti–Al bonds. These graphs summarize the *chemical mechanism* of cleavage in the (100) planes of TiAl.

This observation does not in-and-of itself imply that TiAl is brittle, as we have not determined the mechanism of dislocation nucleation and propagation.

## 3. Conclusion

The mechanism of transgranular cleavage creating (100) surfaces in TiAl can now be summarized in the form of a charge flow diagram. These sort of diagrams have proved useful in the study of other types of reactions. Figure 10 provides such a diagram. We note that the susceptibility of the reaction depicted will be determined by the nearness of the critical points to zero curvature along specified principle axes of the Hessian field. Here these curvatures provide the same information as the relative electrophilicity of the points undergoing charge redistribution in more conventional charge flow diagrams.

With the mechanism of decohesion elucidated, the way is open to study the competing mechanisms of dislocation nucleation and propagation through a similar analysis. Eventually it is hoped that we will be able to qualitatively assess the effects of alloying elements on charge density topology and hence on the mechanisms of decohesion and slip. Such an understanding will provide a rationale for the chemical modification of intrinsic alloy mechanical properties.

**Acknowledgment.** We are grateful to Akzo America for their sponsorship of this research.